Gasoline Spray Characteristics Impinging onto the Wall Surface in Suction Air Flow

Won-Tae Kim
Graduate School of Precision Mechanical Engineering, Chonbuk National University
Shin-Jae Kang*, Byung-Joon Rho
Faculty of Mechanical Engineering, Chonbuk National University

This study investigates the spray characteristics before and after wall impingingment of gasoline spray in suction air flow. For this study, a rectangular model intake port was made of acrylic glass, and suction air was generated by using the forced air blower contrariwise. The injector for this study was a pintle-type port gasoline injector in which an air-assist adaptor is installed to supply assisted air. A PDPA system was employed to simultaneously measure the size and velocity of droplets near the wall. Measured droplets are divided into "pre-impinging droplets" with positive normal velocity and "post-impinging droplets" were negative normal velocity for the suction flow. The velocities, size distributions and Sauter mean diameter (SMD) of pre- and post-impinging droplets for varions injection angles and air-assists are comparatively analyzed.

Key Words : Wall Impingement, Gasoline Spray, Suction Air Flow, Air Assist, Pre-impinging Droplets, Post-impinging Droplets

Nomenclature

d	: Orifice diameter of injector (5mm)
D	: Droplet diameter
$F(D)$	: Number probability density distribution of droplet size
$F(V_n)$	: Number probability density distribution of normal velocity
P_a	: Air assist pressure
V	: Streamwise velocity of suction air
V_n	: Normal velocity of suction air
V_s	: Flow velocity of suction air
X, Y, Z	: Axis of coordinates
θ	: Injection angle of fuel spray

Subscripts

(pre)	: Before impingement
(post)	: After impingement

* Corresponding Author,
E-mail : sjkang@jnplab.chonbuk.ac.kr
TEL : +82-63-270-2387 ; **FAX** : +82-63-270-2472
Faculty of Mechanical Engrg., Chonbuk National University.(Manuscript **Received** November 22, 2000; **Revised** August 10, 2000)

1. Introduction

In the port fuel injection system of gasoline engines, a fuel spray injected into the port impinges onto the surface of the intake valve and the port-wall under a cold start. Then, some fuel droplets, atomized smaller by impingement, bound away from the wall. The other droplets form "wall flows" because fuel droplets cannot be vaporized easily with a "cold" port wall. Some of the wall flows are atomized to small droplets by the fast air flow entrained into the cylinder through the narrow path between the valve and the valve seat in process of suction. However, most are entrained into the cylinder and form nonuniform fuel-air mixture (Kelly-Zion et al., 1995). The nonuniform fuel-air mixture in a cylinder is burned incompletely, resulting in the reduction of combustion efficiency and unburned hydrocarbon emission (Iwano et al., 1991). To solve these problems, the atomization improvement of a fuel injector as well as the fuel injection

under the condition that the suction air flow is occurred, that is intake valve is opening, are considered. The small fuel droplets formed by atomization improvement easily followed the suction air flow into the combustion chamber. Therefore, the unburned hydrocarbon emission is reduced. (Fox et a., 1992). Accordingly, studies that investigate the wall flow visualization (Furuyama et al., 1994) and characteristics of fuel spray (Arcoumanis et al., 1997; Kihm et al., 1995; Wagner et al., 1997; Brenn et al., 1995; Nemecek et al., 1995) in the intake port have been performed. These are, however, limited to the visualization of the spray flow and the investigation of restricted spray characteristics.

In this study, a pintle-type injector which was useful to install the adaptor to supply the assisting air without any manufacturing was used to investigate the characteristics of wall impingement for the spray condition of fuel injected into the intake port. The injector was installed into the model port and assisting air was supplied to improve spray atomization. Moreover, the suction flow velocity was varied to simulate the intake air flow. The injection angle was varied by changing the installed angle of the injector. Droplets were measured by using a PDPA System. The system can simultaneonsly measure droplets velocities and sizes near the impinging wall surface. Measured droplets were them divided into "pre-impinging droplets" with positive normal velocities and "post-impinging droplets" with negative normal velocities, Thus, the droplets velocities, size distributions, and SMD before impingement and after impingement were compared.

2. Experimental Apparatus and Method

2.1 Experimental apparatus

Figure 1 shows the schematic diagram of the experimental set-up for this study. The fuel injector in this study, as shown in Fig. 2, is an air assisted injector. This installs the adaptor for the assisted air to fuel spray using the pintle-type fuel injector employed in the electronic control fuel injection system, MPI (Multi-point injection) system, and combines with the injector housing. An air compressor was employed to pressurize the fuel tank to supply fuel to the injector with a constant pressure. Moreover, some of the pressurized air was used as an air assist through the air inlet of the injector housing. The supplied fuel pressure and the assisted air pressure were measured by a digital pressure converter using the pressure sensor. The fuel injection time and duration were controlled by a computer interfaced through the fuel injection controller.

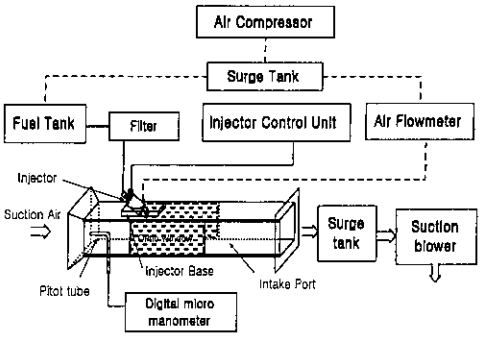

Fig. 1 Schematic diagram of experimental set-up

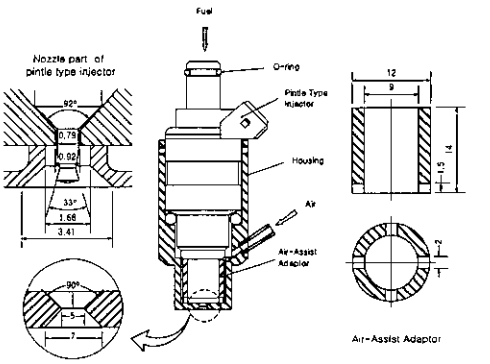

Fig. 2 Configuration of air assist injector

Suction air flow is generated by using a forced air blower contrariwise to simulate the opening condition of the intake valve. A 4-hole pitot tube with a digital micro manometer was inserted into the model intake valve to determine the suction air velocity. The intake port was made of rectangular acrylic glass plate on port, had a 70mm width, 50mm height and 460mm length. A 50mm $\times$170mm optical window was installed on both sides of the model intake port to measure the fuel spray behavior. The PDPA system to measure

droplet size and velocity simultaneously use an air-cooled Ar-ion laser (DANTEC, 300mW). The Bragg cell, which makes it possible to measure the velocity direction as the laser beam transmitted from the laser generator is shifted to 40MHz frequency, is set up in the transmitting optics. The transmitting optics and receiving optics were installed in a fixed bench of three dimensional traverse at 58° and traversed accurately by computer.

2.2 Experimental method

The center of the fuel injector exit is set for origin, and normal direction, streamwise direction of suction air and radial direction of spray flow are set for Z, X and Y respectively, as shown in Fig. 3. The fuel injection duration is set to be 5 ms with an injection pressure of 300kPa. The injection is intermittently made every 100 ms. To improve atomization, fuel spray injection angles are set at 30° and 45°. In addition, the case of non-air assist and the amount of assisted air of a real engine are considered in the air assist adaptor used in this study, The pressure of assisted air is set at 25kPa. Considering the cross section into the intake port and the cross section of the cylinder bore by using the average piston velocity which corresponds to 2800rpm of a small gasoline engine (1500cc), the suction air velocity (V_S) in the port is fixed at 30m/s in this experiment. To investigate the behavior of the spray after impingement onto the bottom of the wall, the spray is measured at an interval of 5 mm from the spray center line of the cross section which is 5mm away from the bottom to the location which is 5mm away from the observation window for the normal direction (Z), and from X/d=10 to X/d=25 for the streamwise direction (X). In this case, the region where the spray does not reach is excluded from the measurement.

3. Results and Discussion

3.1 Spray angle and penetration

Figure 4 shows the spray angle and penetration vs. time after starting injection. A large spray angle is formed early, because the spray length from the front end of the spray is short and the spray is diffused throughout the steady environment. However, the spray angle is suddenly decreased, and then it becomes steady from 4.0 ms after starting injection. In the case of non-air assist, the spray angle is approximately 20° in the steady region after 4.0 ms. At the assisted an supply pressure of 25 kPa, the spray angle is maintained at about 30°. The spray penetration increases linearly for non-air assists, but it increases more due to the momentum increase by the assisted air for air assist. Similar to the study of the air assist fuel injection in the cylinder by Das and Dent (1994), the penetrating distance in this study is proportional to the square root of time.

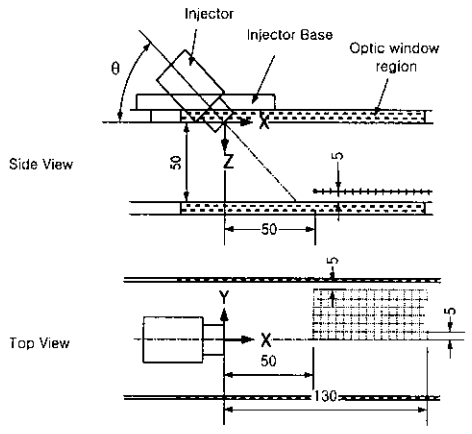

Fig. 3 Measuring points in model intake port

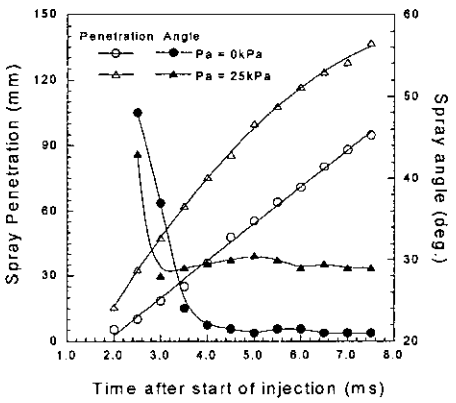

Fig. 4 Variation of spray angle and penetration after start of injection

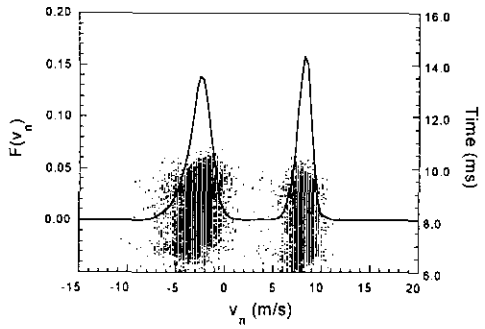

Fig. 5 Distribution of the normal velocity near a wall(X/d=15.0, Z/d=9.0, Y/d=0.0, θ=45°)

3.2 Mean velocity distribution

Figure 5 indicates the probability density distribution and the variation of normal velocity of fuel droplets vs. time after starting the injection of the fuel spray without air assist in the center region (X/d=15.0) of the spray for the suction velocity of 30m/s and spray angle of 45°. Normal velocities of the suction air flow have a high frequency at approximately −2m/s and 8m/s. Furthermore, for the variation of time after starting the injection, fuel droplets which have the negative normal velocity are appeared earlier than which have the positive velocity. Therefore, it can be realized that positive and negative normal velocity obtained at measuring points (X/d=9.0) which are 5mm away from the bottom of the wall are similar to the PDPA data of Nagaoka et al. (1994) obtained it by wall impingement experiment of fuel in the atmosphere to wall impingement numerical analysis of the gasoline spray. It is confirmed that droplets bounced away from the wall after impingement exist considerably, as many droplets which have negative velocity are investigated in the region near the wall.

To analyze more clearly, the probability density distribution of normal velocities of droplets in the spray centerline which is 5 mm away from the impinging wall along the suction air streamwise distance is shown in Fig. 6. These normal velocities of droplets were obtained under the condition of suction air streamwise velocity of 30m/s. In the case of non-air assist, as shown in Fig. 6(a), the peak values of both positive and

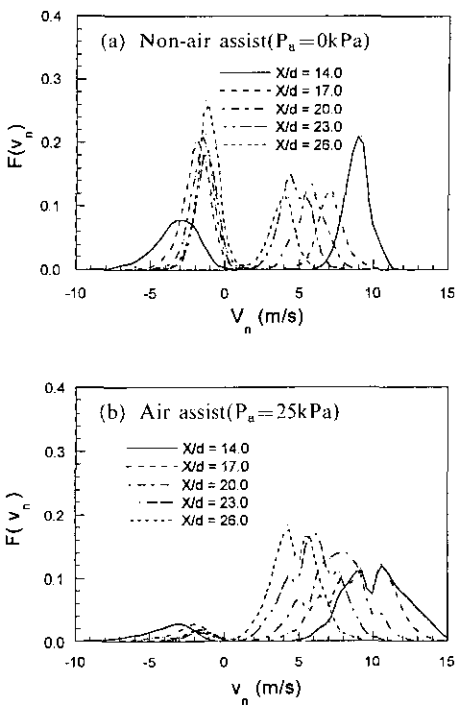

Fig. 6 Number probability density distribution of normal velocity along suction air streamwise distance for spray centerline(θ=45°)

negative normal velocities are investigated at each measuring point. In addition, normal velocities which have the maximum frequency in the negative and positive velocity near the downstream of the suction flow gradually decrease, but the decreasing rate of negative normal velocity is relatively less. Negative normal velocity has a greater frequency than positive except for in X/d =14.0, which means the frequency of measured droplets bounded away after wall impingement increases more than before impingement. For air injection pressure of 25kPa, as shown in Fig. 6 (b), positive normal velocity has a lower maximum frequency but has a wider velocity distribution width compared with the case of non-air assist. Therefore, the small droplets formed by the supply of assisted air have a wide range of the normal velocity distribution. The negative normal velocity distribution also has a similar tendency. Thus, the droplets bounced away from the wall after wall impingement regardless of air-assist.

As can be seen from above, the droplets near

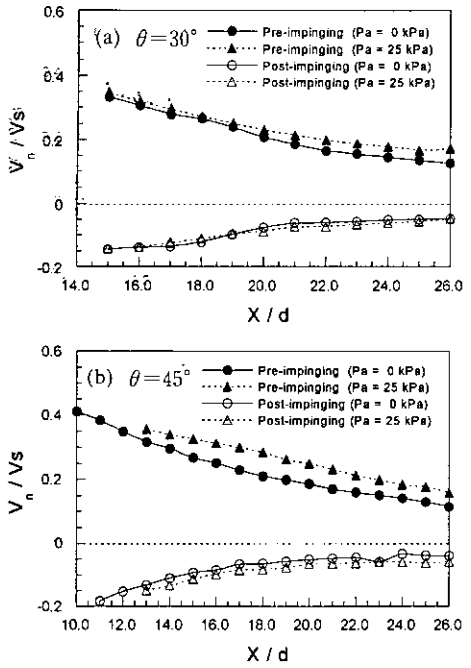

Fig. 7 Mean normal velocity distribution of pre- and post-impinging for spray centerline

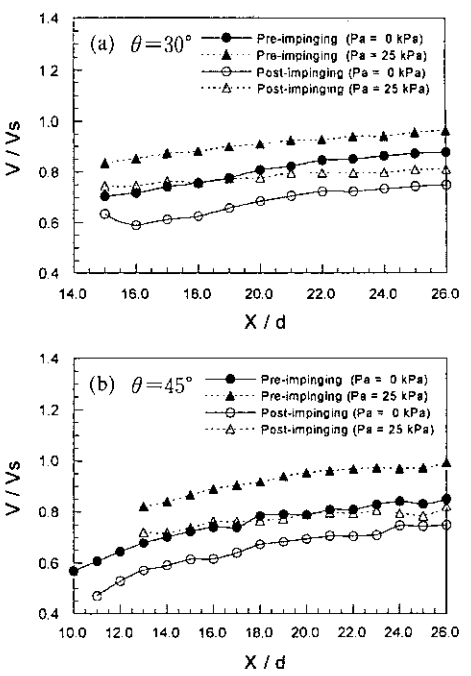

Fig. 8 Mean suction streamwise velocity distribution of pre- and post-impinging for spray centerline

the impinging wall of the spray are clearly divided into droplets with positive normal velocityies and those with negative normal velocityies. Therefore, the former group is defined as "pre-impinging droplets" and the latter is described as "post-impinging droplets".

Figures 7 and 8 indicate the mean normal velocity distribution and the mean suction streamwise velocity distribution of pre- and post-impinging droplets for spray centerline to investigate flow characteristics of pre- and post-impinging droplets at measuring points near the impinging wall under the suction air streamwise velocity of 30m/s. The more the suction air streamwise distance approaches downstream, the more inclined the mean normal velocityies of pre- and post-impinging droplets decrease regardless of injection angle(Fig. 7). The streamwise distance of droplets is altered by the strong suction air flow to that of suction air, as droplets move the downstream. Mean normal velocities of droplets after and before impingement are higher at the injection angle of 45° than at 30°. Furthermore, as injection angle becomes larger, mean normal velocity for air injection pressure of 25kPa has higher values than for non-air assist along the suction air streamwise distance.

Unlike the normal velocity, mean suction air streamwise velocities(Fig. 8), both after and before impingement gradually increase as droplets move downstream. Also, the streamwise velocity decreases as the injection angle goes up. As a result, it is confirmed that the differences in suction air streamwise velocity between pre- and post-impinging droplets along suction streamwise distance are almost uniform irrespective of injection angle and assist-air.

Figure 9 shows the mean velocity ratio of droplets bounded away from the wall after impingement and before impingement along the suction air streamwise distance under each spray condition. Normal velocities of post-impinging droplets are about half as fast as those of pre-impinging droplets for injection angle of 30° and non-air assist, as shown in Fig. 9(a). Also, the mean velocity ratio for air injection pressure of 25kPa is lower than that for non-air assist. However, the

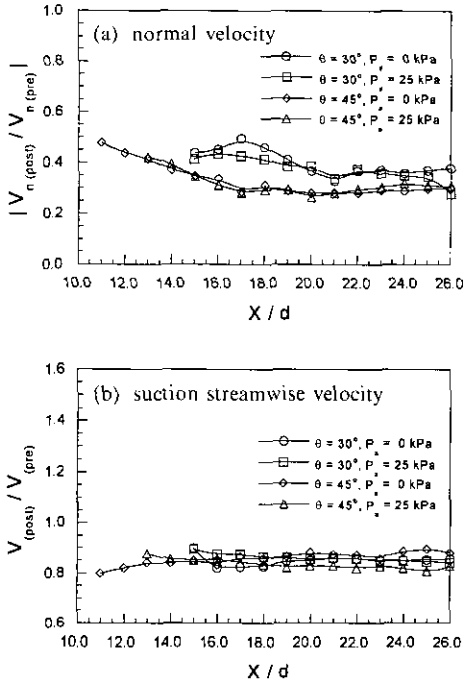

Fig. 9 Mean velocity ratio of pre- and post- impinging for spray centerline

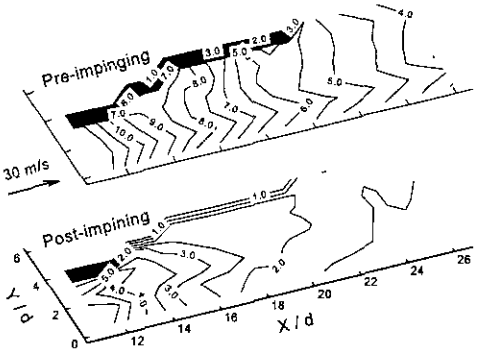

(a) non-air assist(P_a=0kPa)

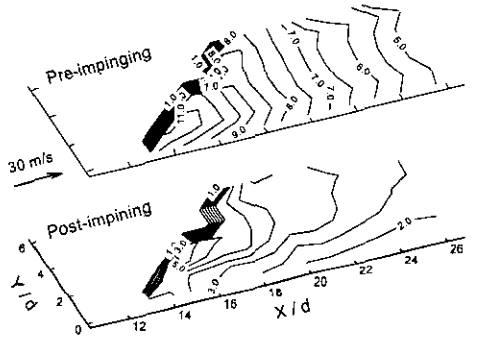

(b) air assist(P_a=25kPa)

Fig. 10 Normal velocity contour for pre- and post- impinging(θ=45°)

difference in mean velocity ratio, between injection pressures of 0kPa and 25kPa, is nearly uniform for injection angle of 45°. In the case of non-air assist, normal velocities of post-impinging droplets maintain high values at 50% of those of pre-impinging in the suction air streamwise distance of the early stage of impingement, but these gradually decrease for the increasement of the distance, and maintain 30% of normal velocity of pre-impinging droplets from X/d=17.0. The suction streamwise velocity distributions (Fig. 9(b)) are uniform (80~90%) along the suction streamwise distance irrespective of injection angle and air-assist. Therefore, it would be expected that normal and suction streamwise velocities of pre- and post-impinging droplets near the wall are affected by the strong suction flow of 30m/s. In addition, it can be confirmed that the difference in mean normal velocity between after and before impingement is maintained uniformly in the downstream region of suction air jets for large injection angles. However, the difference in the mean suction air streamwise velocity is uniform along the suction streamwise distance regardless of injection angle and air-assist.

Figure 10 indicates the normal velocity contour of suction air flow for pre- and post-impinging dropeets at injection angle of 45°. Droplets bounded away from the wall after impingement exist throughout the wider region for θ=45°. The normal velocity distribution of pre-impinging droplets is almost uniform along the lateral direction of the spray regardless of air-assist. As can be considered from above, the normal velocity gradually goes down near the downstream of the suction flow owing to the influence of suction air jets. However, the normal velocities of post-impinging droplets are somewhat different in accordance with their measuring point, but nearly similar.

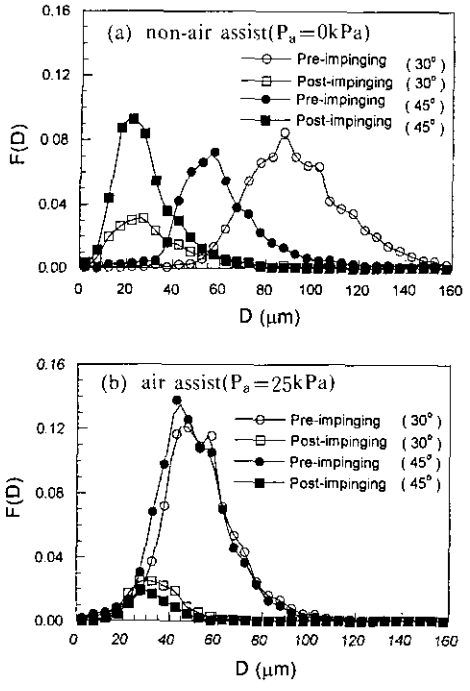

Fig. 11 Number probability density distribution of droplet size for pre- and post-impinging on the spray centerline, X/d=18.0

3.3 Droplet size distribution and SMD distribution

To consider droplet size distribution of pre- and post-impinging droplets, the number probability density distribution of droplet size on the spray centerline at X/d=18.0 is shown in Fig. 11. For the injection angle of 30° and non-air assist (Fig. 11(a)), the peak frequency for the pre-impinging droplets is approximately 85μm, and the large droplets above 150μm are distributed. However, the post-impinging droplets, distribution is the highest near 25μm, and the large droplets between 60 and 100μm are also distributed. For the injection angle of 45° and air-assist, the frequency of small post-impinging droplets in a range of 20~25μm is higher than that of 55~60 μm droplets which have the peak value for pre-impinging. That is, comparing with the case of injection angle of 30°, the distribution of small droplets increases. For the injection angle of 30° and air injection pressure of 25kPa, shown in Fig. 11(b), the droplets between 40 and 60μm have the peak frequency. Post-impinging droplets distribution is the highest near 30μm and droplets in size between 60 and 100μm for non-air assist do not appear. In the case of injection angle of 45°, the post-impinging droplets distribution is quite different from the case of non-air assist in the droplet frequency, and droplets in size above 60μm almost do not exist. Pre-impinging droplet distribution is the highest near 45μm, and its frequency is different compared with the case of injection angle of 45° and air-assist but similar to the post-impinging droplet distribution. Thus, the droplets between 20 and 30μm are mainly distributed by the secondary atomization after impingement. Moreover, small droplets are produced by improvement of atomization for large angles with air assist and they follow the suction air flow well. Therefore, the impinging points of spray front end move to suction streamwise and impinging force that small droplets are received from the wall is small, so that the frequency of droplets bounded away from the wall is dramatically reduced.

Figure 12 shows the droplet size distributions of pre- and post-impinging droplets with air-assist and without air-assist along the suction streamwise distance on the spray centerline (θ=45°). In Fig. 12(a) which represents the case of non-air assist, large size droplets are distributed in the upstream of suction streamwise for pre-impinging. However, small droplets increase downstream because the smaller droplets follow the suction air flow better. Thus, they are moved farther downstream. On the other hand, as shown in the post-impinging droplet size distribution, droplets between 20 and 30μm form the peak frequency irrespective of the suction air streamwise distance, and droplets above 60μm are not distributed almost. The case of pre-impinging dropeets with air-assist pressure of 25kPa (Fig. 12(b)) is similar to Fig. 12(a) except that droplet size and frequency are reduced by air-assist. The small droplets distribution goes up approaching downstream. Droplets above 60μm are not distributed for post-impinging (Fig. 12(b)), which has a similar tendency to the case of non-air assist, Fig. 12(a), except for the decrease of frequency for droplet size. Thus, assisted air im-

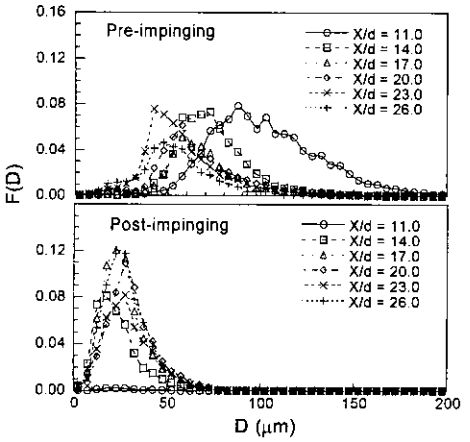

(a) non-air assist(P_a=0kPa)

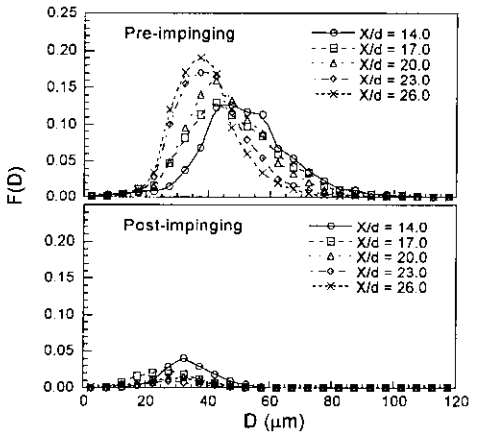

(b) air assist(P_a=25kPa)

Fig. 12 Number probability density distribution of droplet size along suction streamwise distance for the spray centerline(Pa=25 kPa, θ=45°)

proves the atomization of pre-impinging droplets, but does not affect post-impinging droplet droplets significantly.

As shown in Fig. 13, mean droplet diameter is compared by plotting Sauter mean diameters (SMD) distribution for pre- and post-impinging droplets along the suction streamwise distance. For injection angle of 30° and non-air assist in Fig. 13(a), the maximum value of SMD for pre-impinging droplets is 145μm upstream of the suction flow, but it decreases gradually downstream and has a minimum value of 75μm. with injection pressure of 25kPa, SMD is approximately 95μm upstream of the suction flow, but it

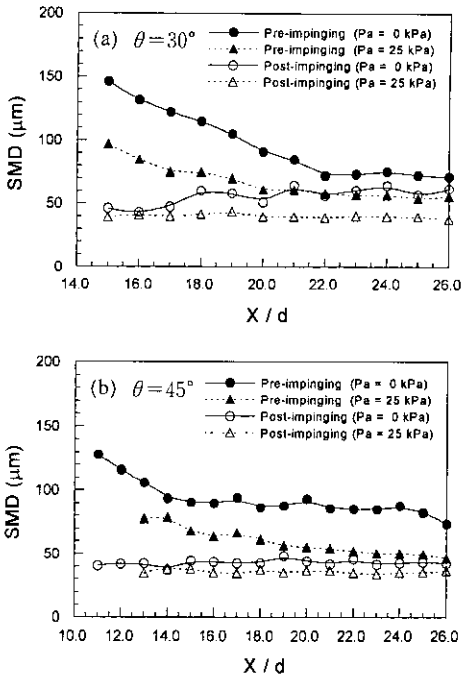

Fig. 13 SMD distribution of pre- and post-impinging for spray centerline

is around 55μm downstream. However, the post-impinging droplets without air-assist have as SMD of approximately 50μm upstream of the spray, and they have a uniform SMD of 60μm downstream, but for air injection pressure of 25kPa have smaller SMD of 40μm. Pre-impinging droplets for injection angle of 45° and non-air assist have an SMD of 130μm upstream of the spray. With air-assist, the SMD is 80μm and it declines gradually approaching downstream. The SMD of post-impinging droplets for air-assist and non-air assist are 35μm 45μm, respectively. As a result, the SMD of post-impinging droplets for the injection angle of 30° and non-air assist upstream of the suction flow decreases to 35% of that of pre-impinging droplets and for air-assist does to 42%. The SMD of post-impinging droplets without air-assist declines by 67% and with air-assist does by 59%. in the case of injection angle of 45°.

The SMD distribution for pre- and post-impinging droplets near the spray impinging wall is plotted in Fig. 14. The SMD distribution of pre-impinging droplets is high in the outer region of

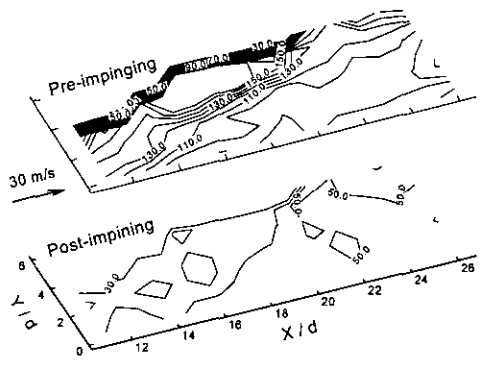

(a) Non-air assist(P_a=0kPa)

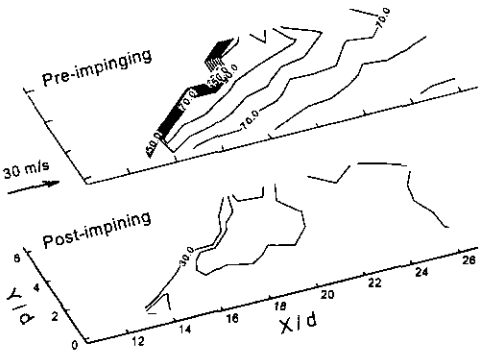

(b) Air assist(P_a=25kPa)

Fig. 14 SMD contour for pre- and post- impinging (θ=45°)

the spray. Post-impinging droplets form a low SMD distribution with nearly uniform sizes due to secondary impingement. Therefore, the secondary atomization improvement by spray wall-impingement is more clear in the outer region of the spray than in the center. In addition, as injection angle is large, the SMD distribution of pre-impinging droplets near the wall is high in the outer region of the spray regardless of air-assist.

4. Conclusions

Pre- and post-impinging droplets are divided by the positive and negative normal velocity distributions, which are obtained by using a PDPA, system. The data are acquired along the suction air streamwise distance near the spray-impinging wall.

As the suction air streamwise distance increases, normal velocities of pre- and post-impinging droplets at the spray centerline gradually decrease due to the effect of suction air. However, the suction streamwise velocity has tends to go up. Moreover, the normal velocities of post-impinging droplets range between 25 and 55% of those of pre-impinging droplets, and is high for the large injection angle. However, this is not quite relative to air-assist. The suction streamwise velocities of post-impinging droplets range between 80 and 90% of those of pre-impinging droplets regardless of injection angle and air-assist.

Without an air-assist, the injection angle has a strong influence on the droplet size distribution, but this effect is halved with air-assist. The number of droplets bounded away after wall-impingement are reduced. This result is clue to the redused momentum of droplets compared with non-air assist, as the atomization of pre-impinging droplets is improved clearly by air-assist. However, their sizes are not changed. The SMD of post-impinging droplets declines by between 58 and 67% of that of pre-impinging droplets owing to the secondary atomization caused by wall-impingement upstream of the suction flow. Also, the SMD reduction is greater for large injection angles and non-air assist in the outer region of the spray.

Acknowledgements

This work was supported by the Research Institute of Industrial Technology in Chonbuk National University.

References

Arcoumanis, C., Whitelaw, D. S., and Whitelaw, J. H., 1997, "Gasoline Injection against Surface and Films," *Atomization and Sprays*, Vol, 5, pp. 417~433.

Brenn, G., Domnick, J., Dorfner, V., Durst, F., and Tremel, P., 1995, "Unsteady Gasoline Injection Experiments: Comparison of Measurements in Quiescent Air and in a Model Intake Port," *SAE 950512*, pp. 1~11.

Das, S. and Dent, J. C., 1994, "A Study of Air-

assisted Fuel Injection into a Cylinder," *SAE 941876*, pp. 1908~1917.

Fox, J. W., Min, K. D., Cheng, W. K., and Heywood, J. B., 1992, "Mixture Preparation in a SI Engine with Port Fuel Injection During Starting and Warm-up," *SAE 922170*, pp. 1088~1099.

Furuyama, M. and Minowa, E., 1994, "Visualization of Intake Port Wall Flow of 4-valve Engines," *JSAE 9432075*, Vol, 25, No. 2, pp. 5~10.

Iwano, H., Jaitoh, M., Sawamoto, K., and Nagaishi, H., 1991, "An Analysis of Introduction Port Fuel Behavior," *SAE 912348*, pp. 1777~1786.

Kelly-Zion, P. L., Deyoung, C. A., Peters, J. E., and White, R. A., 1995, "In-Cylinder Fuel Drop Size and Wall Impingement Measurements," *SAE 952480*, pp. 1~12.

Kihm, K, D., Lyn, G, M., and Son, W. Y., 1995, "Atomization of Cross-injecting Sprays into Convective Air Stream," *Atomization and Sprays*, Vol, 5, pp. 417~433.

Kim, W. T., Lee, S. G., Rho, B. J., and Kang, S. J., 1998, "On the Intermittent Spray Characteristics," *KSME International Journal*, Vol, 12. No. 5, pp. 907~916.

Lee, S. G., Kim, W. T., Rho, B, J., and Kang, S. J., 1998, "Fuel Spray Characteristics Impinging onto the Wall Surface," *Proc. of 4th KSME-JSME Fluids Eng. Conf*. pp. 557~560.

Nagaoka, M., Kawazoe, H., and Namura, N., 1994, "Modeling Fuel Spray Impingement on a Hot Wall for Gasoline Engines," *SAE 940525*, pp. 878~896.

Nemecek, L. M., Wagner, R. M., and Drallmeier, A., 1995, "Fuel Droplet Entrainment Studies for Minimization of Cold-Start Wall-Wetting," *SAE 950508*, pp. 1~11.

Rho, B. J., Kang, S. J., and Kim, W, T., 1999, "A Study on the Spray Behavior of Air-Assist Type Gasoline Fuel Injector in Intake Port," *Transactions of the KSME*, Vol, 23. No. 1, pp. 92~103.

Wagner, R. M., Nemecek, L. M., and Drallmeier, J. A., 1997, "Fuel Delivery in a Port Fuel Injected Spark Ignition Engine," *Atomization and Sprays*, Vol, 7, pp. 629~648.